

EXPERIMENTS WITH HYPERSONIC TURBULENT BOUNDARY LAYERS

ON FLAT PLATES AND DELTA WINGS

By Mitchel H. Bertram,* Aubrey M. Cary, Jr.,**
and Allen H. Whitehead, Jr.**
NASA Langley Research Center
Langley Station, Hampton, Va., U.S.A.

*Head, Hypersonic Fluid Mechanics Branch, Aero-Physics Division, NASA Langley Research Center.

**Aerospace Engineer, Aero-Physics Division, NASA Langley Research Center.

SUMMARY

Recent hypersonic turbulent-boundary-layer experiments and proposed prediction methods pertinent to the problems of the effect of wall temperature on skin friction and heat transfer, the transformation of the compressible boundary layer to the constant-density type, and the heat transfer to delta wings are considered. The level of the turbulent heat-transfer coefficient is found to be little affected by significant changes in wall-temperature level. Coles' transformation as modified by Baronti and Libby has been examined by utilizing turbulent-boundary-layer profiles covering a wide range of Mach number and wall-temperature ratio. Some success is found for the transformation up to the lower end of the hypersonic range and down to moderately low wall-temperature ratios. For delta wings at low angle of attack, in cases where the flow near the surface is essentially streamwise, strip application of successful flat-plate methods gives good predictions of the turbulent heat transfer if the pressures are known. On the lee side of delta wings where vortices are indicated, predictions by strip theory are surprisingly good in general; but predictions can be poor near the center line where the heat transfer is high. Ability to predict the heat transfer to delta wings appears to be contingent upon the ability to predict the flow field.

1. EXPERIMENTS WITH HYPERSONIC TURBULENT BOUNDARY LAYERS

ON FLAT PLATES AND DELTA WINGS

By Mitchell H. Bertram, Aubrey M. Cary, Jr.,
and Allen H. Whitehead, Jr.

INTRODUCTION

The study of the turbulent boundary layer still consists largely of qualitative theory combined with quantitative empiricism. In the present paper, emphasis will be on experimental results. Configurations are considered not for practicality in an engineering sense but to allow the assessment of the basic validity of various prediction methods for skin friction and heat transfer.

Data have been obtained on flat plates, cones, and nozzle walls, so that such a problem as the effect of wall temperature on skin friction and heat transfer can be evaluated. In 1961 Banner, Kuhl, and Quinn (ref. 1) reported heat-transfer experiments at low wall-temperature ratios from X-15 flights which were at variance with the results obtained by prediction methods in use at that time and provoked considerable controversy. Later results from wind tunnels reported by Bertram and Neal (ref. 2) have tended to confirm the trend indicated by the X-15 flight data. Recent experiments bearing on this problem are examined.

Allied to this problem but with the possibility of wider application is the prospect of a transformation for compressible turbulent boundary layers. This approach, which has appealed to investigators for a number of years, is to determine a transformation which, when applied to boundary-layer profiles or other characteristics, will precisely yield the incompressible result. After such a transformation has been obtained, the boundary-layer details are given in terms of the better known incompressible results. Coles has proposed one such transformation which has been modified by Baronti and Libby and examined by them in some detail (ref. 3). This transformation is intended to apply at arbitrary wall temperatures and pressure gradients and, if successful, would provide a tool for determining not only profiles but also skin friction and heat transfer over a wide range of high-speed flow conditions. Recently obtained boundary-layer profiles for extensive values of Mach number and wall temperature, combined with those previously available, allow the determination of the overall validity of the proposed transformation.

Finally, the heat transfer to the more practically shaped delta wing is considered for the case of low angles of attack. Although this wing shape has been dealt with extensively for the laminar case, there is a paucity of data for the turbulent case. Notable exceptions are the results reported in references 4 to 6. In references 4 and 5 the configuration is complicated by considerable leading-edge bluntness.

SYMBOLS

A	constant in law of the wall, taken here to be 2.43
b	constant in law of the wall (taken here to be 7.5) or wing semispan
C_f	local skin-friction coefficient
h	enthalpy
k	vertical height of roughness above plate
M	Mach number
N	exponent
N_{Pr}	Prandtl number
N_{St}	Stanton number
p	static pressure
r	body radius
R	Reynolds number
R_b	Reynolds number based on wing semispan
R_x	Reynolds number based on distance from leading edge or apex
$R_{x,k}$	Reynolds number based on distance to roughness location from leading edge

R_θ	Reynolds number based on boundary-layer-edge conditions and momentum thickness
R_p	Reynolds number based on distance to peak heating
R_v	Reynolds number based on local conditions and distance from peak shear or peak heating
T	absolute temperature
u	velocity
x	distance from leading edge in streamwise direction
x_c	distance from apex of delta wing along root chord
y	distance normal to root chord of delta wing or distance normal to surface for boundary-layer-profile measurements
α	angle of attack of instrumented surface
δ	boundary-layer thickness
δ_k	two-dimensional laminar boundary-layer thickness at roughness location
Λ	leading-edge sweep angle
ν	kinematic viscosity
ρ	density
θ	ray angle from apex of delta wing and root chord
μ	dynamic viscosity
τ	shearing stress
λ_n	leading-edge wedge angle

Subscripts:

aw	adiabatic wall
B-L	from Baronti-Libby method
i	incompressible
l	local conditions
meas	from direct measurement
S-C	from Spalding-Chi method
t	total
v	based on distance from virtual origin
w	conditions at wall
∞	conditions in undisturbed free stream

A bar over a symbol denotes that the variable is in transformed (constant density) flow.

ANALYSIS METHODS

In reducing the data and applying the various prediction methods, the approach was the same as that given in appendix A of reference 2. Although not explicitly mentioned in reference 2, the recovery factor used in reducing the heat-transfer data was as follows. When the recovery factor in the original data reduction was between 0.88 and 0.90, no correction for recovery factor was made. For data in which the recovery factor assumed in the original data reduction was outside these limits, the data were re-reduced by using a recovery factor of 0.89 and all new heat-transfer data were reduced by assuming this recovery factor.

Consistent with the previous paper (ref. 2) the virtual origin for the turbulent boundary layer was chosen as the place where the peak shear or peak heating occurred.

When the Spalding-Chi method (ref. 7) was applied, the values from this method and its modified form were generally taken from the charts given in reference 8. For this case, as well as for the various T' methods (refs. 9 to 11) and the method of Winkler-Cha (ref. 12), the Prandtl number was assumed to be 0.725 for use with the Karman-Reynolds analogy factor. This same Prandtl number was used with the laminar T' method of Monaghan (ref. 13) to obtain values of the laminar-boundary-layer thickness (δ) for defining values of k/δ_k .

In all cases where the ratios $C_f/C_{f,i}$ or $N_{St}/N_{St,i}$ are presented, whether for experiment or for a prediction method, the value of $C_{f,i}$ or $N_{St,i}$ used in the denominator is the Karman-Schoenherr value given in figures 2 and 3 of reference 8.

DISCUSSION

Effect of Wall-Temperature Ratio on Heat Transfer and Skin Friction

Since the time of the X-15 flight data, which was discussed in the "Introduction," a significant body of wind-tunnel results has been obtained. A comprehensive review of available results up to 1965 was presented by Bertram and Neal at a previous AGARD meeting (ref. 2). In results combined from a number of different facilities, general agreement was found with the trend from the X-15 experiments in which wall temperature was indicated to have little effect on the heat-transfer coefficient.

Recently, data have been obtained by A. M. Cary of the NASA Langley Research Center on a sharp flat plate cooled by interior circulation of liquid nitrogen. The plate was precooled outside the nozzle and upon attaining the desired temperature was suddenly plunged into the Mach number 6 airstream of the Langley 20-inch hypersonic tunnel at a preset angle of attack. The findings from this investigation, which are presented in the upper part of figure 1, show little effect of wall cooling on the Stanton number. The experimental trend agrees with that predicted by the Spalding-Chi method (ref. 7) as modified to heat transfer in appendix A of reference 2 and Hank's $\rho_r\mu_r$ method (appendix B of ref. 5). However, the level of the data favors the prediction by the Spalding-Chi method. Clearly the T' or reference temperature methods (refs. 9 to 11) significantly overestimate the heat transfer at the low wall temperatures, and the Winkler-Cha method (ref. 12) underestimates the heating. Examples of the data from which ratios were obtained are given in the lower part of figure 1, where the small scatter indicates the uniformity of the data for a given run and the repeatability of runs.

Further knowledge of the effect of low temperature ratios can be obtained from new work done by Wallace in a shock tunnel at the Cornell Aeronautical Laboratory (ref. 14). In this investigation shots were made at relatively low temperatures and at the lower end of the hypersonic Mach number range to obtain high Reynolds number. Wall temperature was essentially constant at room temperature. Pressure, skin friction, and heat-transfer data were obtained and the sharp flat-plate model was tested in the range of surface incidence from 0° to 20° . Only data from the sharp flat-plate model are considered here and these data were re-reduced from the original tabulation (ref. 15) as follows:

- a. Coefficients and Reynolds number were based on local conditions.
- b. Local conditions were determined from the average of measured wall pressures.
- c. The enthalpy recovery factor was corrected from a value of 1 to a value of 0.89.

The data of Wallace together with some presented by Softley, Graber, and Zempel (ref. 16) are summarized in figure 2, and details are given in figures 3, 4, and 5. For Wallace's data, local Reynolds numbers based on distance from the assumed virtual origin (peak heating) varied from about 10^6 to 2×10^8 . When peak heating occurred ahead of the first measuring station, a value was assumed for the Reynolds number at peak heating that was consistent with the data for which the location of peak heating was known, as shown in figure 6.

Median values of skin-friction and heat-transfer-coefficient ratios obtained by Wallace are shown in figure 2 compared with various prediction methods as in figure 1. The Mach numbers cover the range from 4.5 to 11.7 and the ratio of wall enthalpy to total enthalpy varied from 0.09 to 0.30. Except for the highest Mach number data, the best agreement with experiment is given by the Spalding-Chi theory. As for the Mach 6 results, the prediction of the Monaghan T' method is generally above the data and that of the $\rho_r\mu_r$ method is generally below the data. Whereas the experimental values of the skin-friction and heat-transfer-coefficient ratios are about equal, the $\rho_r\mu_r$ method predicts the values for the skin-friction-coefficient ratio to be significantly less than those for the heat-transfer-coefficient ratio. Examining these data in detail, one finds in figure 3 that the Spalding-Chi method is the only one of those shown that generally matches the level and trend of the shear and heating ratios with Reynolds number.

The highest Mach number data (fig. 2) were anomalous in that the best agreement is with the T' method which appreciably overpredicts all the other data. In this case, the measured wall pressures were 70 to 80 percent of the stream value with the quoted zero plate incidence, as shown in the upper part of figure 4. If the measured pressures are ignored and the pressure ratio is taken as unity, as was done by the authors themselves, there is good agreement of experiment and the Spalding-Chi prediction, as shown in the lower part of figure 4. The choice of these alternatives is unresolved.

There are shown in figure 2 more recent data obtained by Softley, Graber, and Zempel (ref. 16) in a shock tunnel at much the same conditions as the high Mach number results of Wallace (ref. 14). The results in reference 16 were obtained on a 5° half-angle cone and details are given in figure 5. Generally these data are below the Spalding-Chi prediction modified to account for the fact that transition takes place behind the cone apex (appendix B of ref. 2). These data, transformed to the flat-plate case, are presented in figure 2 and together with the Mach 11 Wallace data bracket the Spalding-Chi prediction.

Nerem and Hopkins (ref. 17) from tests in a shock tube have obtained heat-transfer data at h_w/h_{aw} in the range 0.01 to 0.04 at Mach numbers in the 2.5 to 3.5 range. Here, also, reasonable agreement was found between the prediction of Spalding-Chi and the experiments and poor agreement was found with predictions from the Eckert T' method.

The Transformation of Compressible-Boundary-Layer Profiles

One approach to the compressible turbulent-boundary-layer problem which has received considerable attention in recent years has been the effort to find a transformation which, when applied to the compressible turbulent-boundary-layer equations, will yield identically the better-known incompressible turbulent-boundary-layer equations. In this manner the more extensive knowledge for the incompressible turbulent boundary layer can, in theory, be extended to the compressible-flow case of interest. Typical investigations (refs. 18 to 23 and ref. 3) have achieved some measure of success in defining transformations for the turbulent boundary layer. Coles (ref. 23) has proposed an approach to the transformation of the compressible turbulent-boundary-layer equations in which the compressible and the constant-density flows are assumed to be related by three scaling parameters $\sigma(x)$, $\eta(x)$, and $\zeta(x)$. The first parameter relates the stream functions of the two flows, the second is a multiplicative factor of the Dorodnitsyn-Howarth scaling of the normal coordinate, and the third relates the streamwise coordinates of the two flows. An additional assumption pertaining to the invariance of a Reynolds number characterizing the law-of-the-wall region of the boundary layer is necessary to complete the transformation. This assumption, which Coles has called the "substructure hypothesis," provides a substitute for a reference state utilized with many theoretical approaches. Coles' transformation has been extended by Crocco (ref. 22) and modified as well as applied to practical cases by Baronti and Libby (ref. 3). It is with the analysis of Baronti and Libby that the remainder of this section is concerned.

Baronti and Libby modified Coles' substructure hypothesis (they introduced a sublayer hypothesis) and applied the transformation technique by point-by-point mapping of supersonic velocity profiles into the incompressible plane. It should be noted that the transformation theory is applicable only for two-dimensional or axisymmetric ($r \gg \delta$) flow with and without heat transfer or streamwise pressure gradient. This analysis does not define completely the constant-density flow corresponding to the compressible case since the velocity profiles, once transformed, correspond to some unknown \bar{x} -station in the constant-density flow.

Baronti and Libby employed the conventional incompressible equations for the universal velocity profile such that the boundary-layer profile is composed of two distinct regions, a law-of-the-wall region near the wall and a wake or velocity defect region consisting of the major portion of the boundary layer. The equations governing each of these regions, respectively, are:

$$\text{Law of the wall, } \bar{u}/\bar{u}_\tau = f(\bar{\zeta})$$

$$\text{Velocity defect law, } (\bar{u} - \bar{u}_\tau)/\bar{u}_\tau = F(\bar{y}/\bar{\delta}, \bar{x})$$

where

$$\bar{u}_\tau = (\bar{\tau}_w/\bar{\rho}_w)^{1/2}$$

and

$$\bar{\zeta} = \bar{y}\bar{u}_\tau/\bar{v}$$

The law of the wall is conventionally expressed as:

$$\bar{u}/\bar{u}_\tau = \zeta \quad (0 \leq \bar{\zeta} \leq \bar{\zeta}_f \text{ (sublayer)})$$

and

$$\bar{u}/\bar{u}_\tau = A \ln b\bar{\zeta} \quad (\bar{\zeta}_f \leq \bar{\zeta} \leq \bar{\zeta}_1)$$

where $\bar{\zeta}_f$ and $\bar{\zeta}_1$ are the values of $\bar{\zeta}$ at the edge of the laminar sublayer and the outer limit of the region of application of the law of the wall, respectively. The coefficients A and b are 2.43 and 7.5, respectively, as taken from Clauser (ref. 24) so that $\bar{\zeta}_f = 10.6$. The outer limit for the application of the law of the wall is taken as the end of the logarithmic portion of the boundary-layer profile on a scale of \bar{u}/\bar{u}_τ plotted against $\bar{\zeta}$. Simplified equations for the direct application of the Baronti and Libby analysis to velocity profiles for compressible flow may be found in reference 25.

The process of applying the transformation theory through the law of the wall is actually an iterative one, since the value of the skin friction in the incompressible plane is necessary in order to transform the corresponding compressible velocity profile to the incompressible plane. In actual practice the procedure is to assume values of the wall skin friction in an incompressible plane until acceptable agreement of the velocity profile with the constant-density result is achieved. The success of the transformation may then be judged by observing how well the transformed velocity profile correlates with the incompressible results and comparing the resulting compressible-skin-friction estimate with that measured or predicted by a reliable theory. Once the incompressible skin friction has been determined from the law-of-the-wall analysis, a comparison with the velocity-defect law is directly obtainable.

Baronti and Libby applied the transformation to velocity profiles for compressible flows up to Mach 9 for adiabatic wall and moderate heat-transfer conditions. In general, their results indicated good correlation of the compressible velocity profiles for the law of the wall in the incompressible plane, and the values of skin friction resulting from the transformation compared well with those measured in most of the investigations cited. However, when a correlation was attempted with the velocity-defect law, the results indicated that a compressible velocity profile under a uniform flow would transform into the incompressible plane and show the characteristics of an incompressible velocity profile under the influence of a pressure gradient. Tennekes (ref. 26) has suggested that this discrepancy may be a result of a distortion of the velocity-defect region of the boundary layer by the Dorodnitsyn-Howarth density scaling of the normal coordinate.

Here the same procedures that were used by Baronti and Libby were used to reduce the compressible velocity profiles to the incompressible form, including the use of the Crocco relation to calculate the density integral through the boundary layer, but the range of Mach number and heat transfer is extended. Experimental velocity profiles were calculated by using measured temperature profiles where available; otherwise the Crocco relation was used. Illustrations of the correlation of the transformed compressible boundary-layer profiles according to the law of the wall with the classical incompressible results are shown in figure 7. Since C_f was not directly measured for most of the profiles presented, the skin-friction results obtained from the transformation for all the cases were normalized by the skin-friction coefficient predicted by the method of Spalding and Chi (ref. 7). In each case, the Spalding-Chi prediction was based on the measured R_θ and T_w/T_t .

The transformation of profiles obtained on tunnel walls in nominal zero-pressure-gradient flow as shown in figure 7(a) provides good correlation for Mach numbers from 2.5 to 8.¹ The skin-friction results from these profiles compare favorably with the Spalding-Chi predictions. For still higher Mach numbers, in the range from 15 to 20, the profiles shown in figure 7(b) appear to correlate well with the incompressible results, but the extent of the logarithmic part of the law-of-the-wall region of the profile is small in comparison with the lower Mach number profiles.² An inspection of the compressible velocity profiles indicates that, in general, as Mach number increases, the laminar sublayer thickness as well as the extent of the wake or velocity-defect region becomes larger. As a result, there appears to be a corresponding decrease in the extent of the logarithmic law-of-the-wall region. Since the wall shear obtained from the transformation is dependent upon a curve fit in the logarithmic law-of-the-wall region, a physical limit of the application of the transformation in the present form may thus exist. However, for profiles with thick laminar sublayers for which sublayer velocity measurements are accurate, the transformation could be applied directly in conjunction with the sublayer part of the law of the wall. The skin-friction results from the transformation of the high Mach number profiles show more deviation than those for the lower Mach number profiles. It should be remarked that the nitrogen profile presented in figure 7(b) is believed to be transitional by the experimenters (ref. 28). However, note that there is no particular difference between this transformed profile and the other presented at considerably higher values of R_θ .

Most of the profiles presented thus far are for moderate values of wall-temperature ratio. Transformed profiles for Mach numbers near 7 (ref. 14) and low values of wall-temperature ratio are given in figure 7(c). Correlation is as good as was found for the previous profiles in figure 7(a), but the resulting values of skin friction are significantly greater than Spalding-Chi predictions.

An illustration of the effect of previous history of the boundary layer on the results of the transformation is shown in figure 7(d). The transformed profiles correlate nicely, and the skin-friction results compare favorably with the predictions of Spalding and Chi, even though each of the boundary layers developed under different conditions.

A compilation of the skin-friction results obtained from the transformation technique is presented in figure 8(a). The skin-friction results from the transformation are referenced to the skin friction predicted by the Spalding-Chi method and presented as a function of the ratio of wall temperature to total temperature for each particular case. The data include all the experiments analyzed by Baronti and Libby, results cited in figure 7, and additional results from references 29 to 32. It has been shown in several investigations (for example, ref. 2 and in the first section of this

¹Mach 2.49 and 4.44 profiles from unpublished measurements by Stallings and Couch in the Langley Unitary wind tunnel; Mach 6.0 and 6.8 from reference 2; Mach 7.95 from unpublished measurements by W. V. Feller in Langley 18-inch variable-density wind tunnel, all with dp/dx essentially zero.

²Mach 15.6 profile from reference 27; Mach 20.2 profile from reference 25; Mach 18.4 profile from unpublished measurements by W. D. Harvey and F. L. Clark but a similar profile is found in reference 28.

paper) that the method of Spalding and Chi can be expected to give accurate skin-friction predictions on flat plates and cones at least up to Mach 9 and over the entire range of T_w/T_t for the data in figure 8.

In general, the skin-friction results from the transformation appear to be consistently higher than those predicted by the Spalding-Chi method. Although the overprediction is in the 10-percent range for adiabatic and moderately cooled walls, the error is large for extreme cooling conditions. Wallace (ref. 14) obtained direct skin-friction measurements on the nozzle wall at the same locations and the same flow conditions for which the profile data were taken. The measured skin-friction results shown in figure 8(b) are in good agreement with the Spalding-Chi predictions, as are the results from other investigations in which direct measurements of skin friction were made. It thus appears that the transformation as applied is not generally valid even for the logarithmic portion of the law of the wall.

Since in the application of the transformation theory it is necessary to define a temperature distribution through the boundary layer (the Crocco distribution for both this investigation and that of Baronti and Libby), it may be suspected that the particular distribution assumed would affect the skin friction obtained from the transformation. Thus, it is believed reasonable to examine some of the available temperature distributions in detail. A number of measured temperature profiles were presented in reference 2. Since that time some additional profiles have become available and these are shown in figure 9. The upper part of figure 9 is from reference 2, which presents data from references 29 and 33 to 36 with the addition of unpublished measurements obtained by R. L. Stallings and L. M. Couch in the Langley Unitary wind tunnel. These experimental profiles are compared with the suggested profiles of Crocco, Michel (ref. 37), and Walz (ref. 38). There is disagreement between the data of references 34 and 35 on one hand and the data of references 29, 36, and Stallings and Couch on the other. The former sets of data agree more closely with the Crocco and Michel prediction and the latter sets agree more closely with Walz' prediction.

Some relatively cold wall data are shown in the lower part of figure 9 from reference 39 and unpublished measurements obtained by W. V. Feller in the Langley 18-inch variable-density wind-tunnel. These data do not agree with any of the prediction methods previously shown and depart considerably from nonlinearity. This is also seen in the profiles presented in figures 18 and 19 of reference 2. A better fit to experiment, as shown in figure 9, would be a profile which had a quadratic form

$$\frac{T_t - T_w}{T_{t,\infty} - T_w} = \left(\frac{u}{u_w}\right)^2$$

This is equivalent to assuming that Walz' adiabatic wall-temperature distribution is independent of wall-temperature ratio.

Since the quadratic temperature profile represents experimental results better than the Crocco profile, at least at low wall-to-total-temperature ratios, the transformation was applied by using the quadratic temperature profile for several compressible profiles with low wall-to-total-temperature ratios. For each case the quadratic temperature law was applied in both the reduction of the pitot profile to velocity and in the transformation. The transformed results from one Wallace profile (Mach 7.61, fig. 7(c)) and one by Harvey and Clark (Mach 18.4, fig. 7(b)) exhibited poor correlation with the incompressible results, and the agreement of the resulting skin-friction coefficients with the Spalding-Chi predictions was no better than was found by using the Crocco relation. The Wallace profile at Mach 7.21 (fig. 7(c)) when transformed by use of the quadratic law did yield a skin-friction coefficient in good agreement with Spalding-Chi, but again poor correlation of the transformed profile was obtained with the incompressible results.

Thus, these limited results indicate that the quadratic profile offers little improvement over the approach of Baronti and Libby. The discrepancy in wall shear at low wall-to-total-temperature ratios does not appear to be a function of Mach number or Reynolds number and may result from a deficiency in the transformation theory itself. A true test of the validity of the theory in the low wall-to-total-temperature range will require more extensive data than that presented here.

Heat Transfer to Delta Wings at Low Angles of Attack

The delta planform is of interest as a practical shape wing for hypersonic flight purposes. For efficient flight, the angle of attack will be low and for the large air-breathing vehicles the leading-edge size necessary from aerothermodynamic considerations is small compared with wing chord. Here, the essentially idealized case of wings with sharp leading edges will be treated.

Consider the wing shown in figure 10(a), on which tests were made at zero angle of attack by Whitehead in the Mach 6 airstream of the Langley 20-inch hypersonic tunnel. (Part of this study was reported in ref. 40.) The cross section of the wing tested was actually half-diamond with the flat side instrumented and aligned with the flow. The shock was attached to the leading edge and the pressure ratio on the instrumented surface was essentially unity. Stanton number is shown as a function of Reynolds number and the boundary-layer flow is indicated to be transitional at the most forward measuring stations. If the virtual origin of the turbulent boundary layer is taken to be at the location of peak heating, the assumption of strip-like flow which is successful with laminar boundary layers is found to give a good prediction for turbulent flow over this delta wing. When this wing is inclined so that the instrumented surface faces 5° to the windward ($k/\delta_k \approx 2.2$), the shock remains

attached and the pressures are within 5 to 10 percent of the two-dimensional shock value as shown in conical coordinates in figure 10(b). As for the zero angle-of-attack case, the Stanton number is predicted within about 10 percent by strip theory, figure 10(b), using the predicted two-dimensional pressure.

Using two different wings at zero inclination to the flow, Murray and Stallings (ref. 6) were able to obtain data under conditions where the leading-edge shock was attached and detached. The attached-shock case occurs for a 60° swept delta wing at Mach 4.4 and is shown to the left in figure 11, and the detached-shock case occurs for a 70° swept delta wing at Mach 3 and is shown to the right in figure 11.³ In the upper part of figure 11, the heating and pressure data are shown as a function of streamwise Reynolds number and in the lower part of the figure in terms of ray angle. The heat-transfer parameter is chosen to correlate the heating data with the virtual origin of the Reynolds number (R_v) at the location of the boundary-layer trips. For simplicity, a power law for heat transfer was chosen which fitted the Spalding-Chi theory for the conditions of the test and the exponent from this fit was used in the heat-transfer correlation in figure 11.

Leading-edge shock detachment on the 70° swept wing is caused by a bevel on the under side. The pressures show a behavior typical of a subsonic cross flow where the stagnation point is on the beveled under side, and the pressure drops sharply as the flow expands around the sharp leading edge. Using the conical coordinate gives good correlation of the pressures measured on the wing surface, whereas using the linear coordinate gives poor correlation. The surface on which the pressures are measured is flat and aligned with the flow, but the pressures are as low as 50 percent of free-stream pressure at the most forward stations.

Oil flow in the same stream on a 70° swept wing with a smaller leading-edge bevel angle (also with a detached shock) indicated surface flow lines were essentially parallel to the root chord. This suggests using the modified Spalding-Chi method in stripwise fashion with local values of correlated experimental pressures. A good prediction of the heat transfer was obtained and is shown in the lower right side of figure 11. However, if the pressures had not been available and the surface pressure had been taken as equal to free-stream pressure, a significant error would have been incurred in heat-transfer predictions over much of the wing, as shown in figure 11.

At Mach 4.4, for the 60° swept wing there is a slight pressure gradient which may be due to warping of the model during the test. If the Spalding-Chi method is applied in the stripwise manner previously used, a good prediction of the heating is obtained when presented on a chordwise basis rather than conical as shown on the upper left side of figure 11.

The heat-transfer data at the most forward position show a trend which is different from the rest of the data. This behavior is believed caused by proximity to the oversize roughness. (A similar effect is shown on flat plates in ref. 41.)

Again consider the wing tested by Whitehead in the Mach 6 airstream. With the flat instrumented side of the wing facing leeward at the angle of 5° to the free stream, the shock is calculated to be attached. However, only a small deflection of the wing under load would suffice to cause leading-edge shock detachment. The pressures, shown in the right-hand side of figure 12, do not vary much over the span and appear to correlate well in conical coordinates with no particular difference in the pressure distribution between the case where the surface is smooth and the case where spherical boundary-layer trips ($k/\delta_k \approx 1.1$) are placed on the surface near the leading edge.

Without boundary-layer trips, the heat transfer to this surface was transitional only at the rearmost stations of the near root chord region. With spherical trips, the level of aerodynamic heating was increased to a general level expected with turbulent flow, as shown on the left-hand side of figure 12. In this case, Stanton number is shown as a function of Reynolds number based on free-stream conditions and distance from the leading edge parallel to the root chord. For reference purposes, the modified Spalding-Chi method was applied in stripwise fashion for a constant pressure on the wing equal to the two-dimensional value. (The virtual origin is taken as $R_{w,x} = 2 \times 10^6$, based on the indicated peak in heating along the root chord.) If the prediction method applied, then one would not expect more than about 20 percent difference, based on the variation in the pressures, between prediction and experiment. Clearly, there is no correlation of the data and there are large increases in heat transfer in the midportion of the wing where surface-oil-flow studies indicate a conical vortex system to be formed. (See ref. 40.) As in the previous presentation, the main body of the heat-transfer data appears to correlate in the conical coordinate as shown on the upper right-hand side of figure 12. The large increase in heating is seen to be confined to the central region of the wing influenced by the vortex system and referred to as the "feather" region in reference 40. Apparently, no increase in pressure is associated with this increase in heat transfer. However, there is a gap in the pressure data and such an increase in pressure may have occurred over a very narrow range of ray angle. If this pressure increase does exist at 5° angle of attack, the extent of the increase probably widens with angle of attack. (The pressure increase was seen on the lee side when the model was positioned at 10° angle of attack, as shown in fig. 13 of ref. 40.)

An analysis of the delta-wing data of reference 6 at Mach numbers from 3 to 4.4 and 5° angle of attack, windward and leeward, shows a similar behavior to the Mach 6 data previously presented in

³Test conditions: At $M_\infty = 4.44$, $T_t = 687^\circ \text{ R}$ and $k/\delta_k = 3.1$.

At $M_\infty = 2.98$, $T_t = 711^\circ \text{ R}$ and $k/\delta_k = 4.4$.

figures 10 and 12. These results are shown in figure 13 and indicate that the level of the heating on the lee side can approach that on the windward side near the center of the wing. Better coverage of the central region of the lee surface is needed to determine just how high the heating actually is.

CONCLUDING REMARKS

Recent hypersonic turbulent-boundary-layer experiments and proposed prediction methods pertinent to the problems of the effect of wall temperature, the transformation of the compressible boundary layer to a constant-density type, and heat transfer to the delta wing have been considered.

Up to a Mach number of at least 9, based on flat-plate experiments, the level of the turbulent heat-transfer coefficient is found to be little affected by significant changes in wall temperature, as was predicted by the Spalding-Chi method. The T' or reference-temperature method overpredicts skin friction and heat transfer at low wall-temperature ratios.

The Coles' transformation as modified by Baronti and Libby has been examined by utilizing turbulent-layer profiles covering a wide range of Mach number and wall-temperature ratio. Some success is found for the transformation up to the lower end of the hypersonic range and down to moderately low wall-temperature ratios. However, at the lowest wall-temperature ratios, the transformation gave high wall shears as compared with Spalding-Chi predictions and with shears that were actually measured. At high Mach numbers, very little of the logarithmic portion of the transformed profile remains because of an apparent thickening of the sublayer adjacent to the wall and the velocity-defect wake region comprising the outer part of the profile. It is the logarithmic portion of the profile from which the indicated shear is obtained.

Delta-wing turbulent heat transfer has been examined for several types of flow. At low angles of attack, in cases where the flow near the surface is essentially streamwise, strip application of successful flat-plate methods gives good predictions of the heat transfer if the pressures are known. This result applies whether the leading-edge shock is attached or detached. On the lee side of delta wings where vortices are indicated, predictions by strip theory are surprisingly good in general; but predictions can be poor near the center line where the heat transfer is high. Success in predicting the heat transfer to delta wings appears to be contingent upon the ability to predict the flow field.

REFERENCES

1. Banner, Richard D.; Kuhl, Albert E.; and Quinn, Robert D.: Preliminary Results of Aerodynamic Heating Studies on the X-15 Airplane. NASA TM X-638, 1962.
2. Bertram, Mitchel H.; and Neal, Luther, Jr.: Recent Experiments in Hypersonic Turbulent Boundary Layers. NASA TM X-56335. Presented at the AGARD Specialists' Meeting on Recent Developments in Boundary Layer Research Sponsored by the Fluid Dynamics Panel of AGARD, Naples, Italy, May 10-14, 1965.
3. Baronti, Paolo O.; and Libby, Paul A.: Velocity Profiles in Turbulent Compressible Boundary Layers. AIAA J., vol. 4, no. 2, Feb. 1966, pp. 193-202.
4. Paulsen, James J.; and Schadt, Gail H.: A Study of the Pressure and Heat Transfer Distribution on Highly Swept Slab Delta Wings in Supersonic Flow. AIAA Paper No. 66-130, Jan. 1966.
5. Nagel, A. L.; Fitzsimmons, H. D.; and Doyle, L. B.: Analysis of Hypersonic Pressure and Heat Transfer Tests on Delta Wings With Laminar and Turbulent Boundary Layers. NASA CR-535, 1966.
6. Murray, William M., Jr.; and Stallings, Robert L., Jr.: Heat-Transfer and Pressure Distributions on 60° and 70° Swept Delta Wings Having Turbulent Boundary Layers. NASA TN D-3644, 1966.
7. Spalding, D. B.; and Chi, S. W.: The Drag of a Compressible Turbulent Boundary Layer on a Smooth Flat Plate With and Without Heat Transfer. Jour. Fluid Mech., vol. 18, pt. 1, Jan. 1964, pp. 117-143.
8. Neal, Luther, Jr.; and Bertram, Mitchel H.: Turbulent-Skin-Friction and Heat-Transfer Charts Adapted From the Spalding and Chi Method. NASA TN D-3969, 1967.
9. Monaghan, R. J.: On the Behaviour of Boundary Layers at Supersonic Speeds. Fifth International Aeronautical Conference, Rita J. Turino and Caroline Taylor, eds., Inst. Aeron. Sci., Inc. 1955, pp. 277-315.
10. Eckert, E. R. G.: Engineering Relations for Friction and Heat Transfer to Surfaces in High Velocity Flow. J. Aero. Sci., vol. 22, no. 8, Aug. 1955, pp. 585-587.
11. Sommer, Simon C.; and Short, Barbara J.: Free-Flight Measurements of Turbulent-Boundary-Layer Skin Friction in the Presence of Severe Aerodynamic Heating at Mach Numbers From 2.8 to 7.0. NACA TN 3391, 1955.
12. Winkler, Eva M.; and Cha, Moon H.: Investigation of Flat Plate Hypersonic Turbulent Boundary Layers With Heat Transfer at a Mach Number of 5.2. NAVORD Rept. 6631, U.S. Naval Ord. Lab., Sept. 15, 1959.
13. Monaghan, R. J.: An Approximate Solution of the Compressible Laminar Boundary Layer on a Flat Plate. R & M No. 2760, British A.R.C., 1956.
14. Wallace, J. E.: Hypersonic Turbulent Boundary Layer Studies at Cold Wall Conditions. 1967 Heat Transfer and Fluid Mechanics Institute (San Diego, Calif.), June 19-21, 1967.
15. Heronimus, G. A.: Hypersonic Shock Tunnel Experiments on the W7 Flat Plate Model - Expansion Side, Turbulent Flow and Leading Edge Transpiration Data. CAL Rept. No. AA-1952-Y-2 Contract No. AF 33(615)-1847, Feb. 1966.
16. Softley, E. J.; Graber, B. C.; and Zempel, R. E.: Transition of the Hypersonic Boundary Layer on a Cone. Part 1 - Experiments at $M_\infty = 12$ and 15. General Electric Report R67DS39, November 1967. Part of this paper presented at the AIAA 6th Aerospace Sciences Meeting, Jan. 1968 as AIAA paper No. 68-39.
17. Nerem, Robert M.; and Hopkins, Richard A.: An Experimental Investigation of Heat Transfer From a Highly Cooled Turbulent Boundary Layer. Presented at the AIAA Sixth Aerospace Sciences Meeting, AIAA Paper 68-43, Jan. 22-24, 1968.
18. Burggraf, O. R.: The Compressibility Transformation and Turbulent-Boundary-Layer Equations. J. Aerospace Sci., vol. 29, no. 4, April 1962, pp. 434-439.
19. Mager, Artur: Transformation of the Compressible Turbulent Boundary Layer. J. Aeron. Sci., vol. 25, no. 5, May 1958, pp. 305-311.
20. Spence, D. A.: Velocity and Enthalpy Distributions in the Compressible Turbulent Boundary Layer on a Flat Plate. J. Fluid Mech., vol. 8, pt. 3, July 1960, pp. 368-387.
21. Coles, Donald E.: Measurements in the Boundary Layer on a Smooth Flat Plate in Supersonic Flow, III. Measurements in a Flat-Plate Boundary Layer at the Jet Propulsion Laboratory. Jet Propulsion Laboratory, Rept. No. 20-71 (Contract No. DA-04-495-Ord 18), Jet Propulsion Lab., California Inst. Technol., June 1, 1953.

22. Crocco, L.: Transformations of the Compressible Turbulent Boundary Layer With Heat Exchange. AIAA J., vol. 1, no. 12, Dec. 1963, pp. 2723-2731.
23. Coles, D. E.: The Turbulent Boundary Layer in a Compressible Fluid. U.S. Air Force Project RAND Rept. R-403-PR, The RAND Corp., Sept. 1962.
24. Clauser, F. H.: Turbulent Boundary Layers in Adverse Pressure Gradients. J. Aeron. Sci., vol. 21, no. 2, Feb. 1954, pp. 91-108.
25. Watson, Ralph D.; and Cary, A. M., Jr.: The Transformation of Hypersonic Turbulent Boundary Layers to Incompressible Form. AIAA J. (Tech. Notes), vol. 6, no. 6, June 1967, pp. 1202-1203.
26. Tennekes, H.: Law of the Wall for Turbulent Boundary Layers in Compressible Flow. AIAA J., vol. 5, no. 3, Mar. 1967, pp. 489-492.
27. Henderson, A., Jr.; Rogallo, R. S.; Woods, W. C.; and Spitzer, C. R.: Exploratory Hypersonic Boundary-Layer Transition Studies. AIAA J. (Tech. Notes), vol. 3, no. 7, July 1965, pp. 1363-1364.
28. Clark, Frank L.; Ellison, James C.; and Johnson, Charles B.: Recent Work in Flow Evaluation and Techniques of Operation for the Langley Hypersonic Nitrogen Facility. Fifth Hypervelocity Techniques Symposium, Denver Res. Inst. and Arnold Eng. Develop. Center, Mar. [16-17], 1967, vol. 1 - Advanced Experimental Techniques for Study of Hypervelocity Flight, pp. 347-373.
29. Lobb, Kenneth R.; Winkler, Eva M.; and Persh, Jerome: NOL Hypersonic Tunnel No. 4 Results VII: Experimental Investigation of Turbulent Boundary Layers in Hypersonic Flow. NAVORD Rept. 262, Mar. 1955.
30. Samuels, R. D.; Peterson, J. B., Jr.; and Adcock, J. B.: Experimental Investigation of the Turbulent Boundary Layer at a Mach Number of Six With Heat Transfer at High Reynolds Numbers. NASA TN D-3858, 1967.
31. Sterrett, J. R.; and Barber, J. B.: A Theoretical and Experimental Investigation of Secondary Jets in a Mach 6 Free Stream With Emphasis on the Structure of the Jet and Separation Ahead of the Jet. Presented at the Separated Flows Specialists' Meeting Fluid Dynamics Panel - AGARD, Brussels, Belgium, 1966.
32. Maddalon, D. V.; Rogallo, R. S.; and Henderson, A., Jr.: Transition Measurements at Hypersonic Mach Numbers. AIAA J. (Tech. Notes), vol. 5, no. 3, Mar. 1967, pp. 590-591.
33. Reynolds, W. C.; Kays, W. M.; and Kline, S. J.: Heat Transfer in the Turbulent Incompressible Boundary Layer. I - Constant Wall Temperature. NASA MEMO 12-1-58W, 1958.
34. Kistler, Alan L.: Fluctuation Measurements in Supersonic Turbulent Boundary Layers. BRL Report No. 1052, Aberdeen Proving Ground, Aug. 1958.
35. Nothwang, George J.: An Evaluation of Four Experimental Methods for Measuring Mean Properties of a Supersonic Turbulent Boundary Layer. NACA Rept. 1320, 1957. (Supersedes NACA TN 3721, 1956.)
36. Adcock, Jerry B.; Peterson, John B.; and McRee, Donald I.: Experimental Investigation of the Turbulent Boundary Layer at $M = 6$ and High Reynolds Numbers at Zero Heat Transfer. NASA TN D-2907, 1964.
37. Michel, R.; and Mentré, P.: Quelques Resultats sur les Caracteristiques Thermiques des Couches Limites Turbulentes a Temperature Elevee. AGARDograph 97, Recent Developments in Boundary Layer Research, Part 1, May 1965.
38. Walz, A.: Compressible Turbulent Boundary Layers. Int'l. Symp. on The Mechanics of Turbulence, Marseilles, France, Aug. 28-Sept. 2, 1961, Centre Nat'l de la Reserche Scienficque, N. Y., Gordon and Breach 1964, pp. 299-350.
39. Scaggs, Norman E.: Boundary Layer Profile Measurements in Hypersonic Nozzles. ARL 66-0141, U.S. Air Force, July 1966.
40. Whitehead, Allen H., Jr.; and Keyes, J. Wayne: Flow Phenomena and Separation Over Highly Swept Delta Wings With Trailing Edge Flaps at Mach 6. Presented at the AIAA Sixth Aerospace Sciences Meeting. AIAA Paper 68-97, Jan. 22-24, 1968.
41. Sterrett, J. R.; Morrisette, E. L.; Whitehead, A. H., Jr.; and Hicks, R. M.: Transition Fixing for Hypersonic Flow. NASA TN D-4129, 1967.

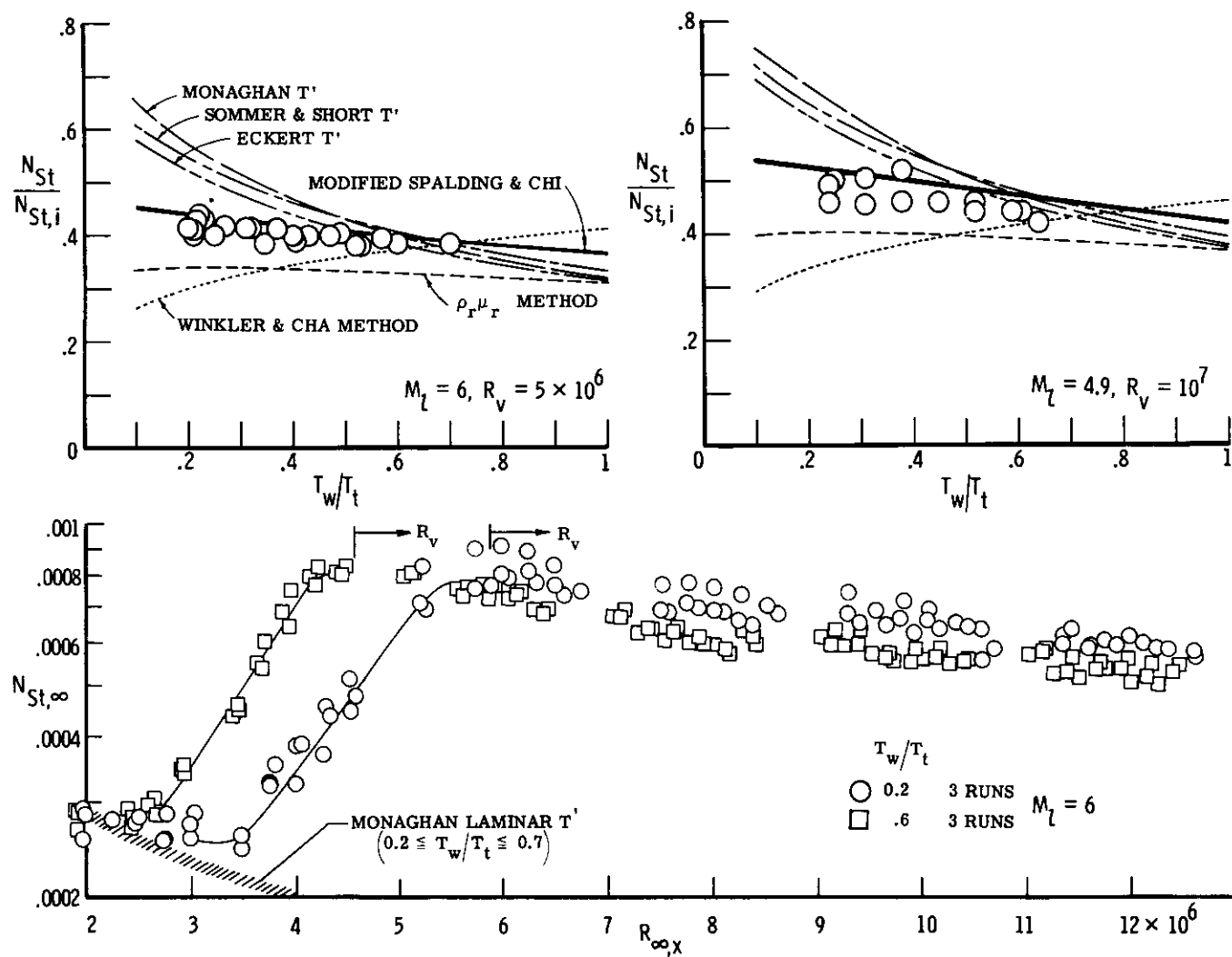


Figure 1.- Effect of wall temperature on turbulent heat transfer to a sharp flat plate at $M_\infty = 6$. $R_\infty/\text{in.} = 0.67 \times 10^6$; $T_t = 960^\circ \text{R}$.

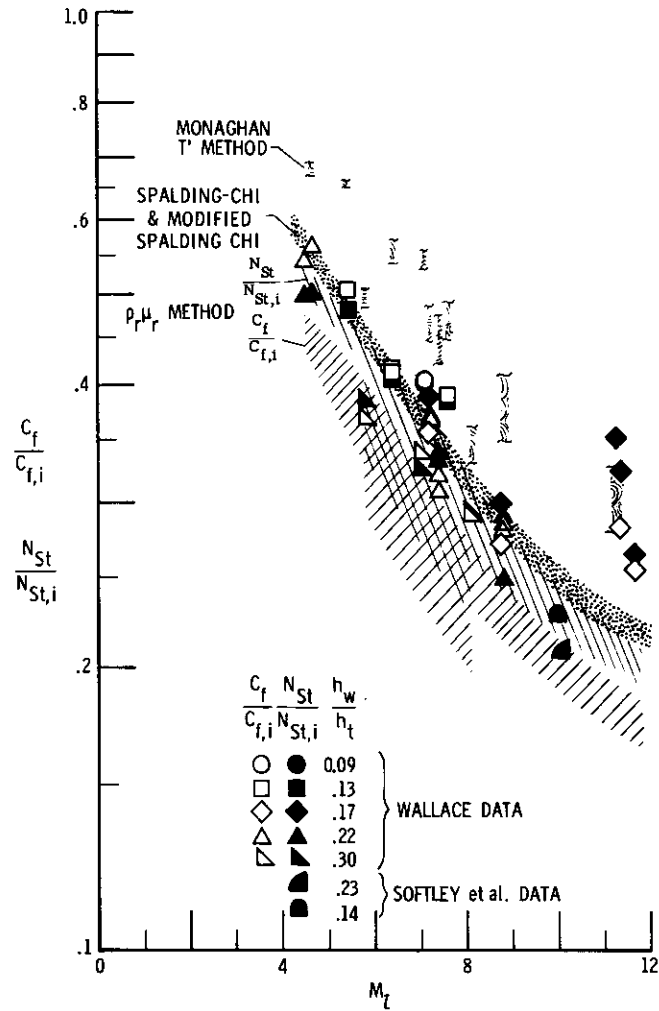


Figure 2.- Comparison of cold-wall turbulent skin-friction and heat-transfer results with prediction methods.
 $T_w \approx 530^\circ \text{ R.}$

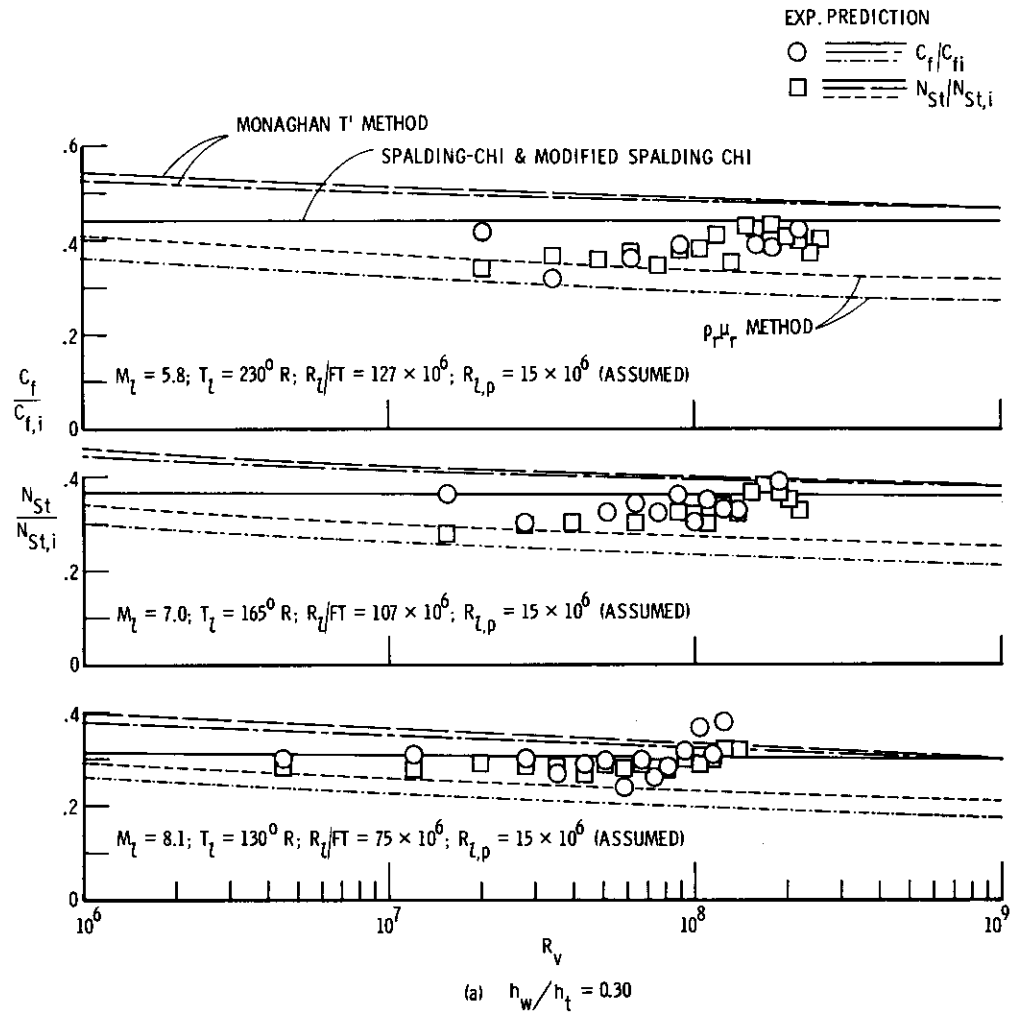


Figure 3.- Detailed comparison of Wallace's turbulent sharp flat-plate skin-friction and heat-transfer data with various prediction methods.

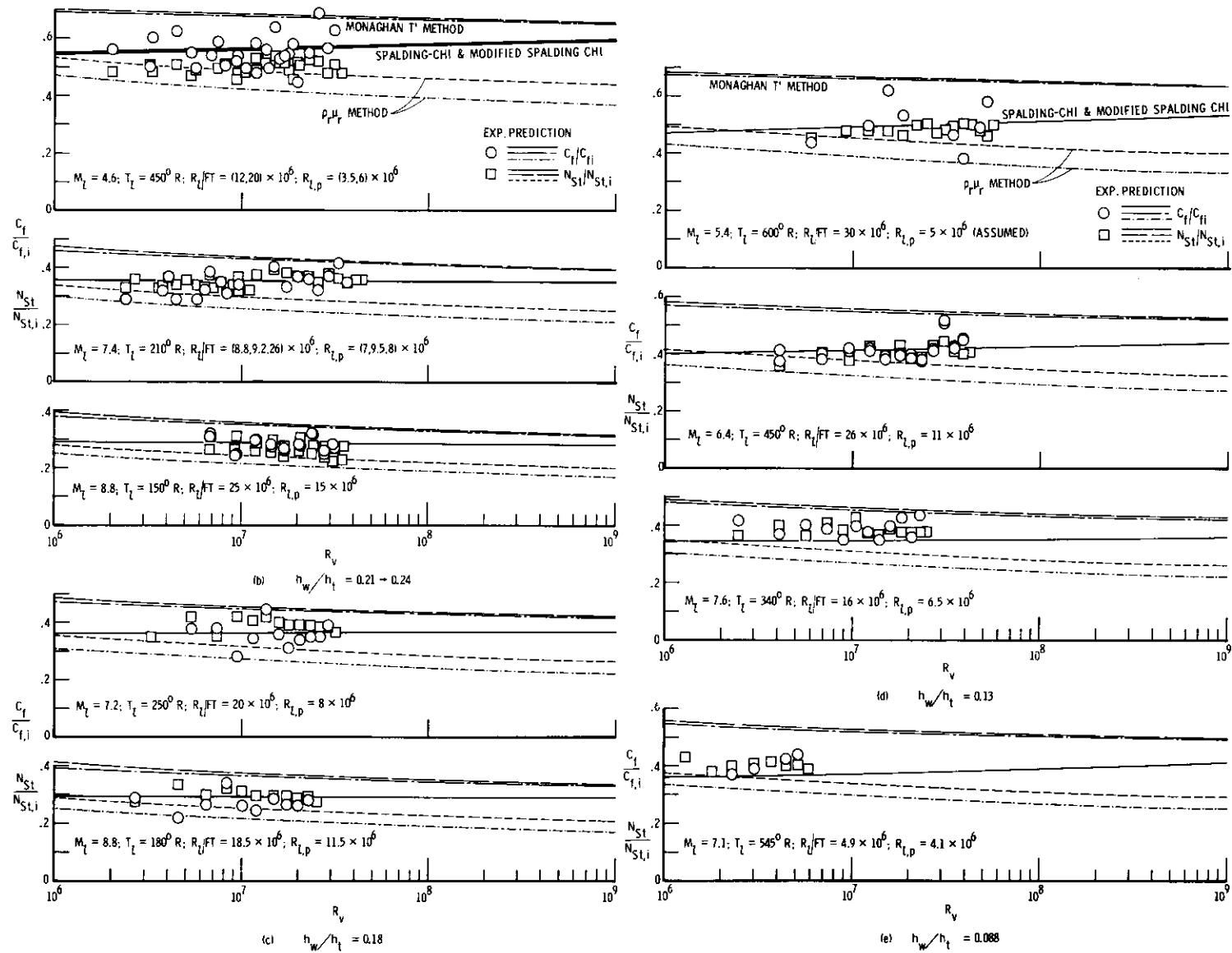


Figure 3.- Concluded.

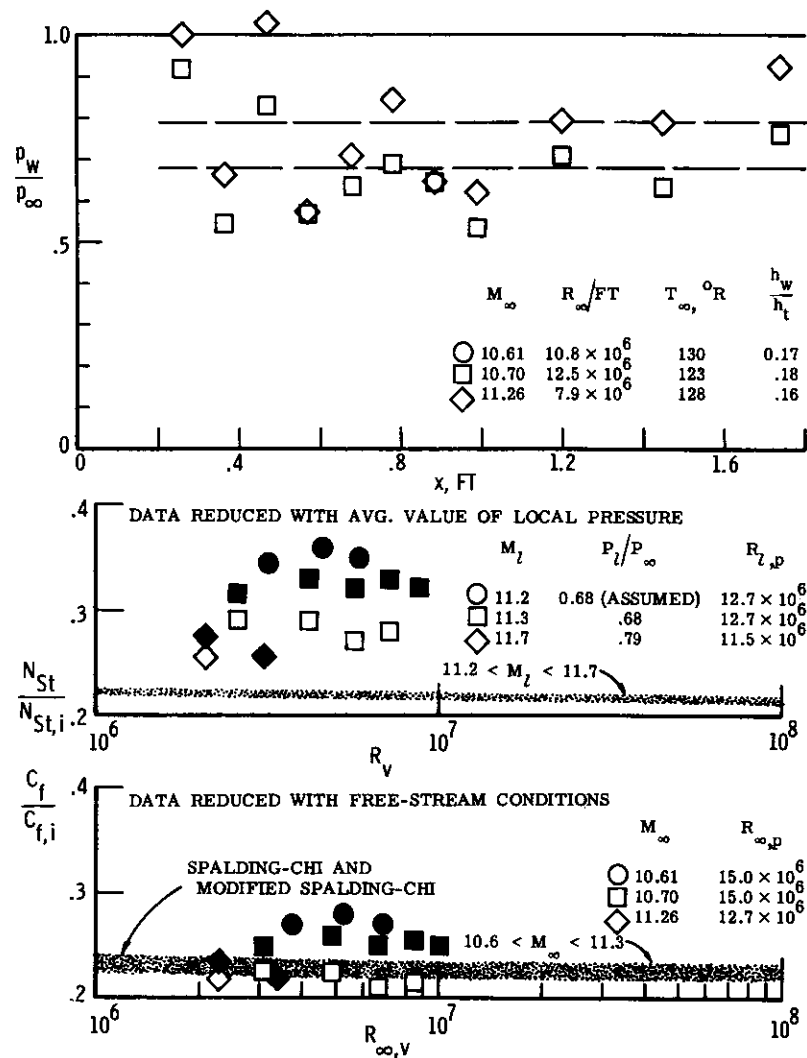


Figure 4.- Analysis of Wallace's highest Mach number turbulent data.

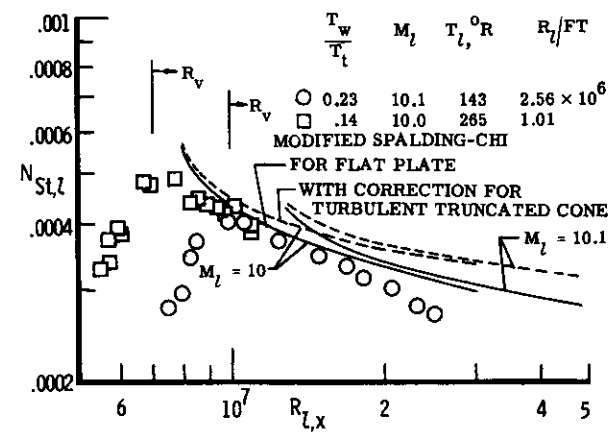


Figure 5.- Softley, Graber, and Zempel data from a cone. $\theta_c = 5^\circ$.

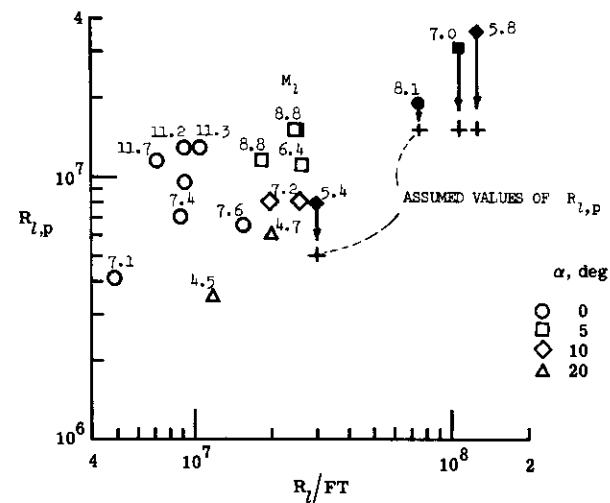


Figure 6.- Values of Reynolds number for peak heating used as virtual origin for Wallace's turbulent data.

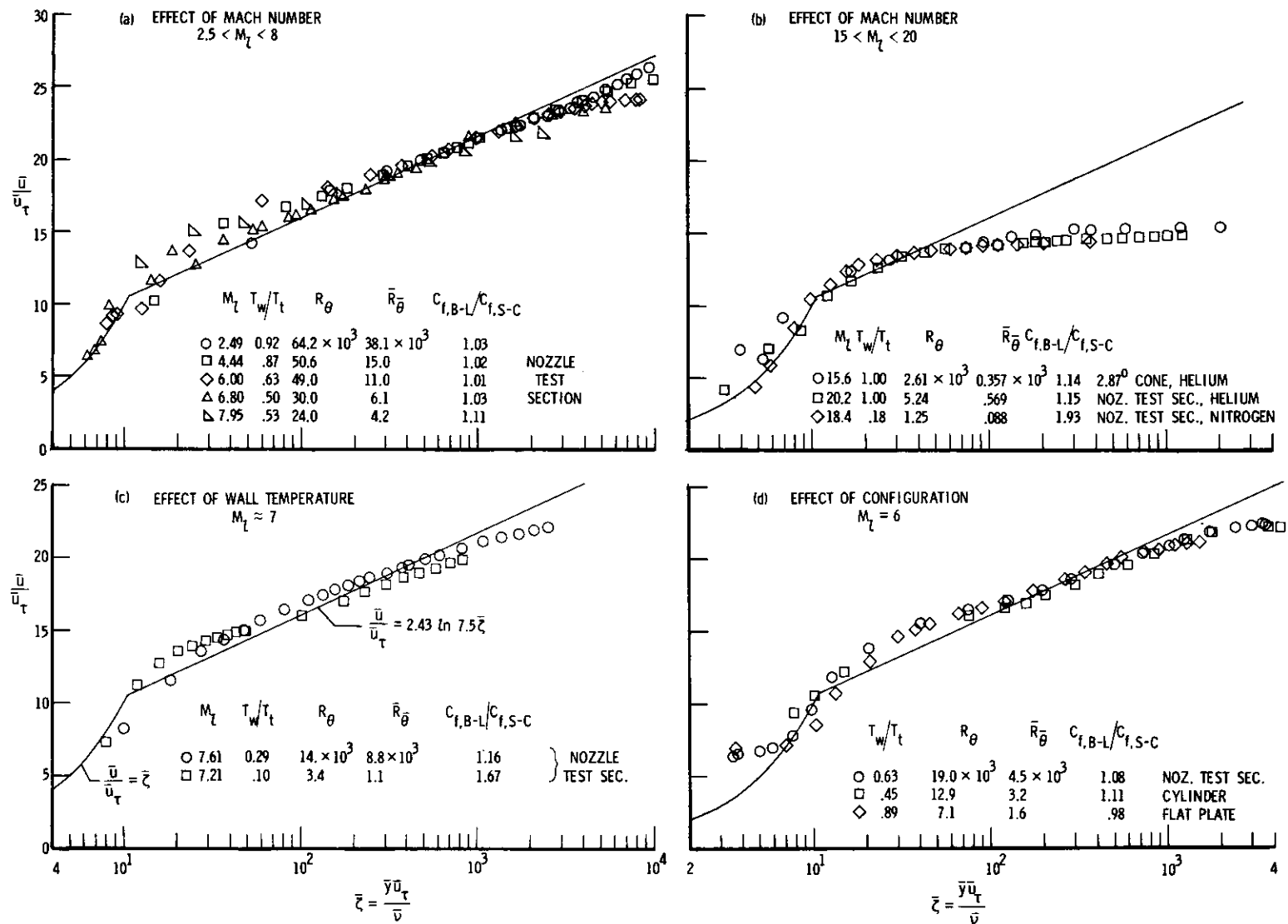


Figure 7.- Compressible turbulent velocity profiles in the incompressible plane according to the transformation of Coles and of Baronti and Libby.

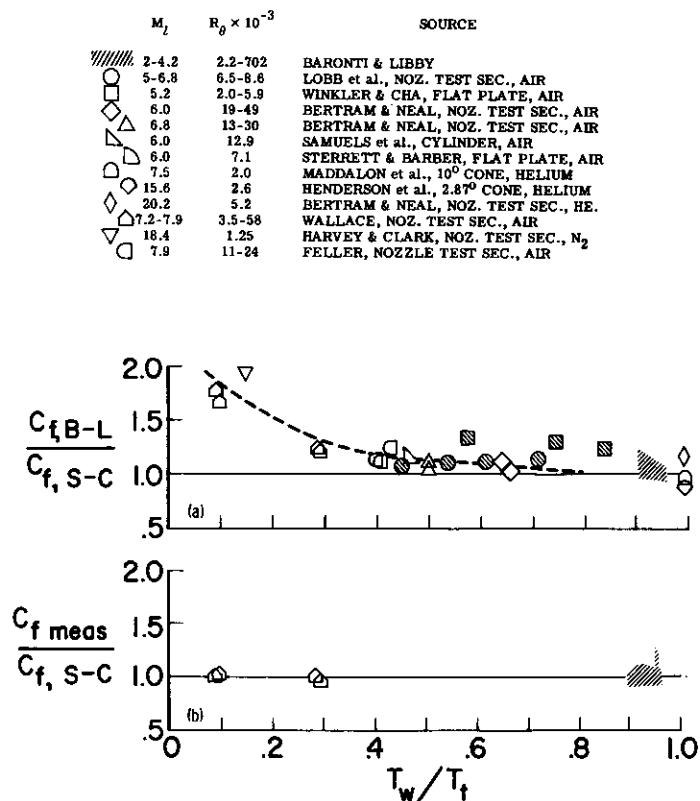


Figure 8.- Local skin friction from the Baronti-Libby transformation and from direct measurements at the same location.

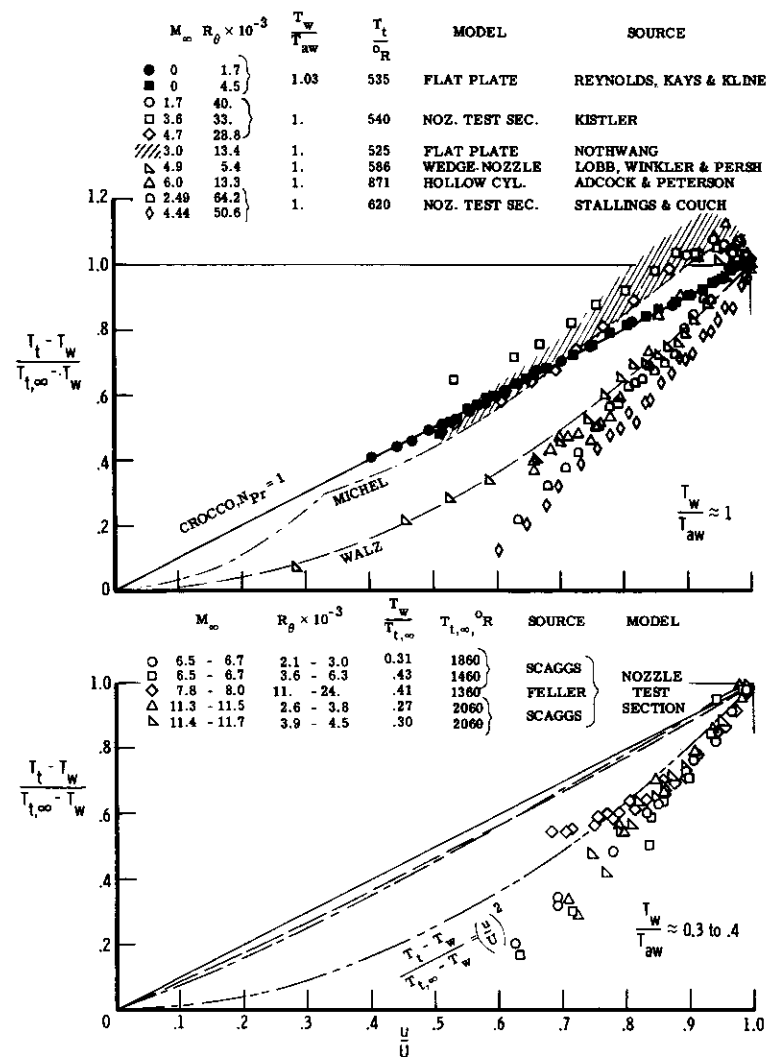


Figure 9.- Turbulent temperature-velocity profiles.

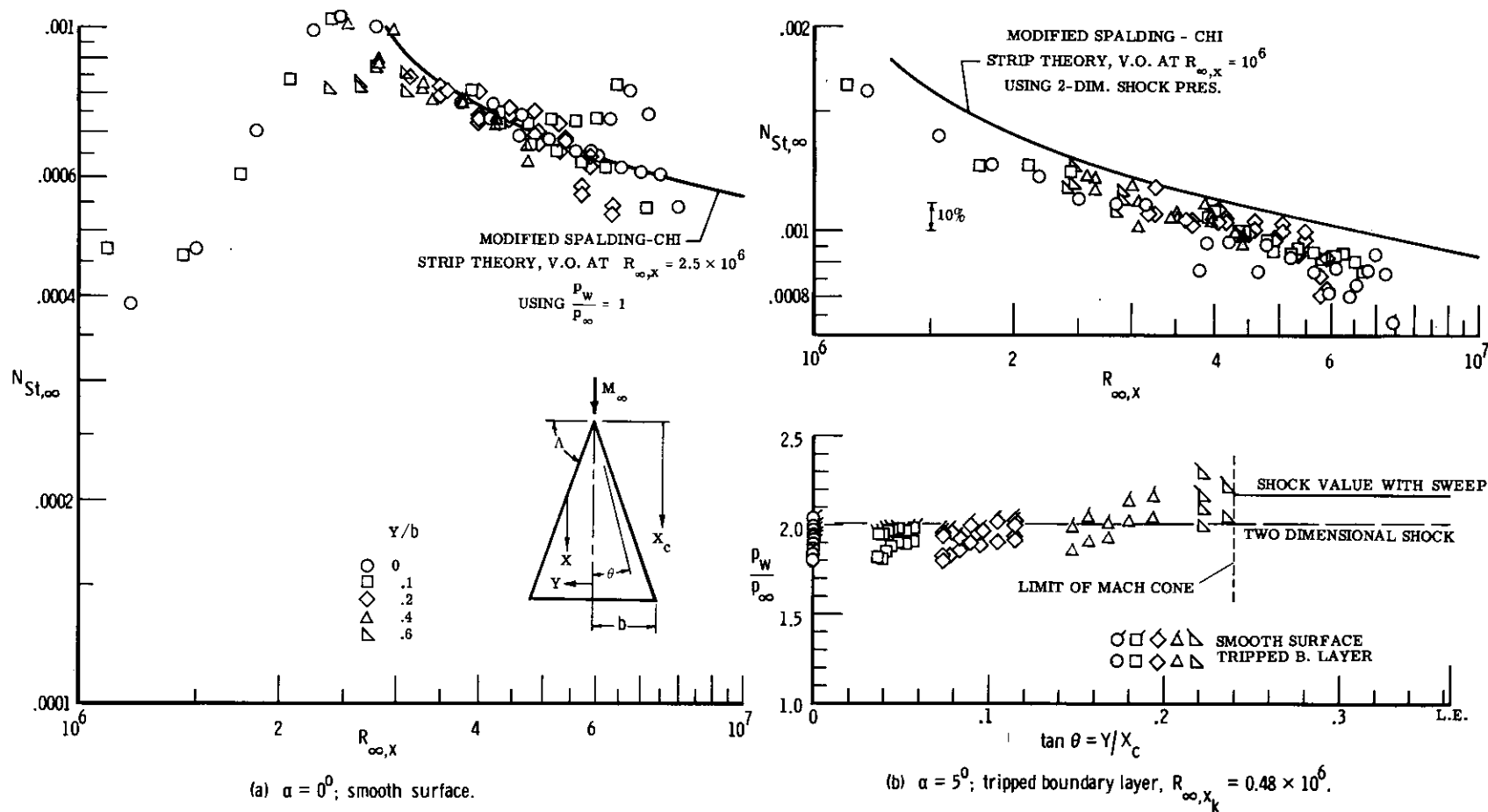


Figure 10.- Turbulent heat transfer to flat surface of a sharp delta wing at $M_\infty = 6$. $\Lambda = 70^\circ$; $T_t = 960^\circ \text{ R}$; $T_w/T_t = 0.6$; $R_{\infty,b} = 2.7 \times 10^6$; $b = 4.91 \text{ in}$. Shock attached to leading edge; $\lambda_n = 9.25^\circ$.

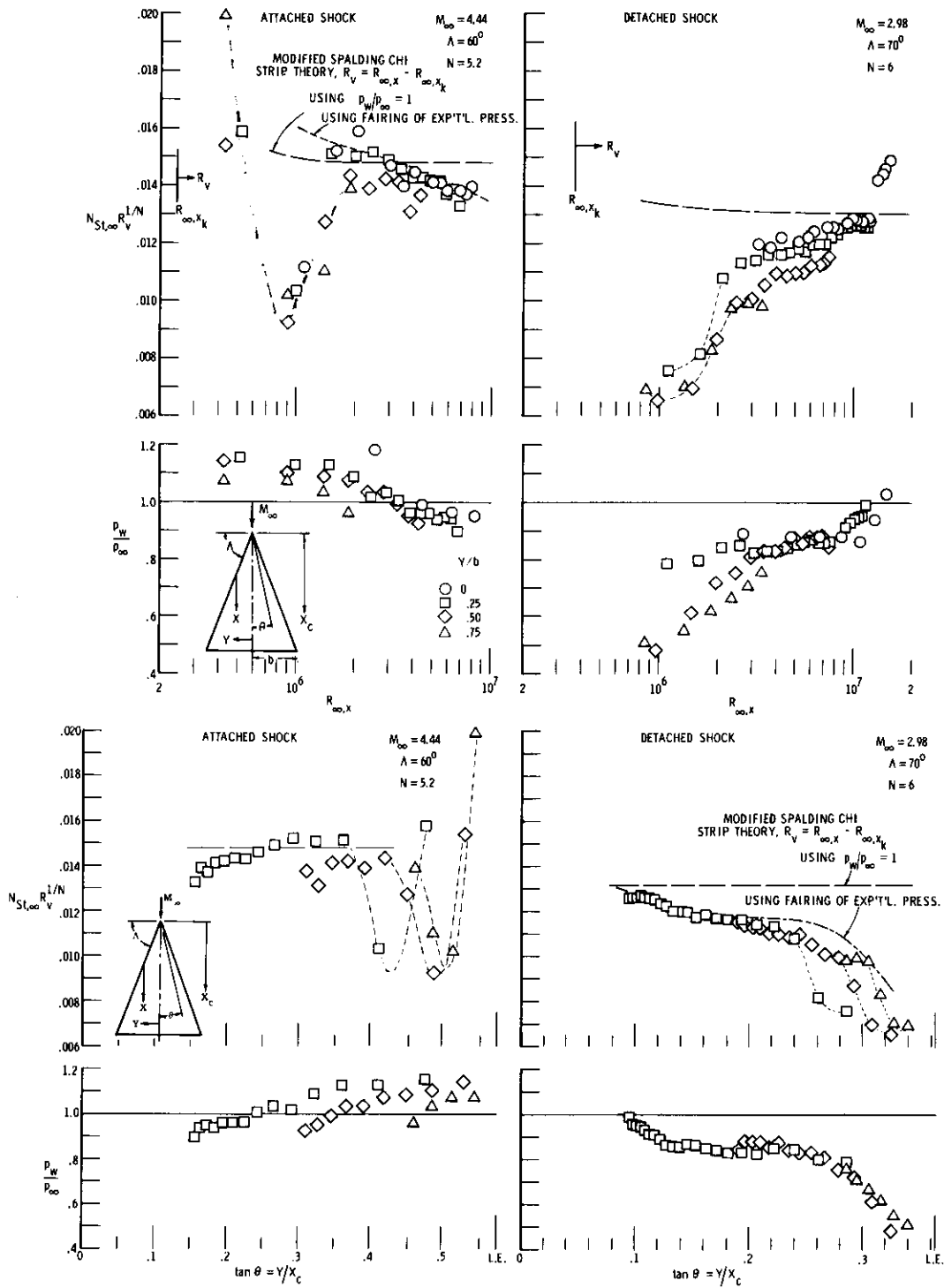


Figure 11.- Turbulent heat transfer and pressure distribution on sharp flat delta wings; $\alpha = 0^\circ$; $T_w/T_t = 0.83$; $b = 12$ in.; $\lambda_n = 15^\circ$. Data from NASA TN D-3644.

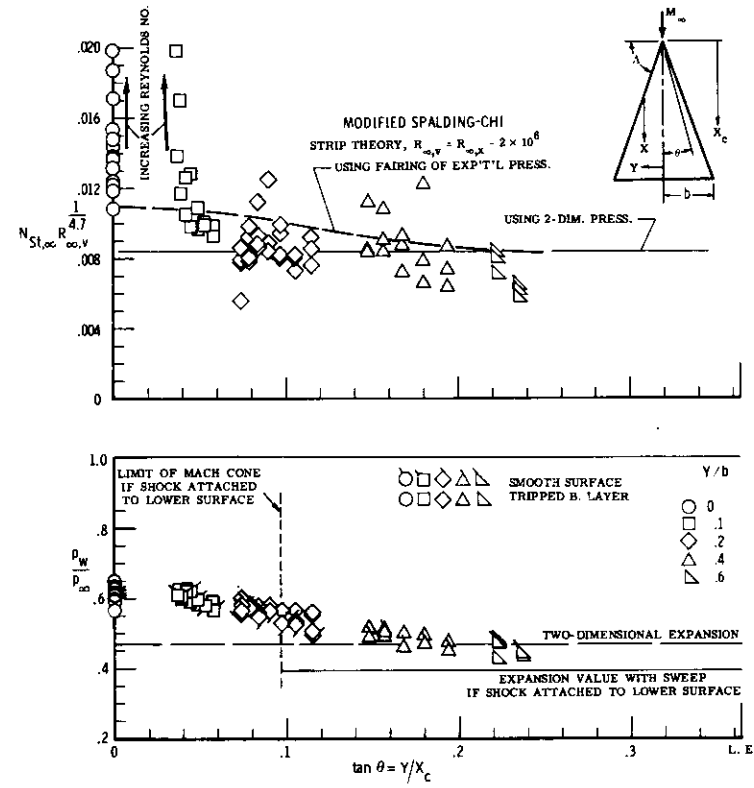
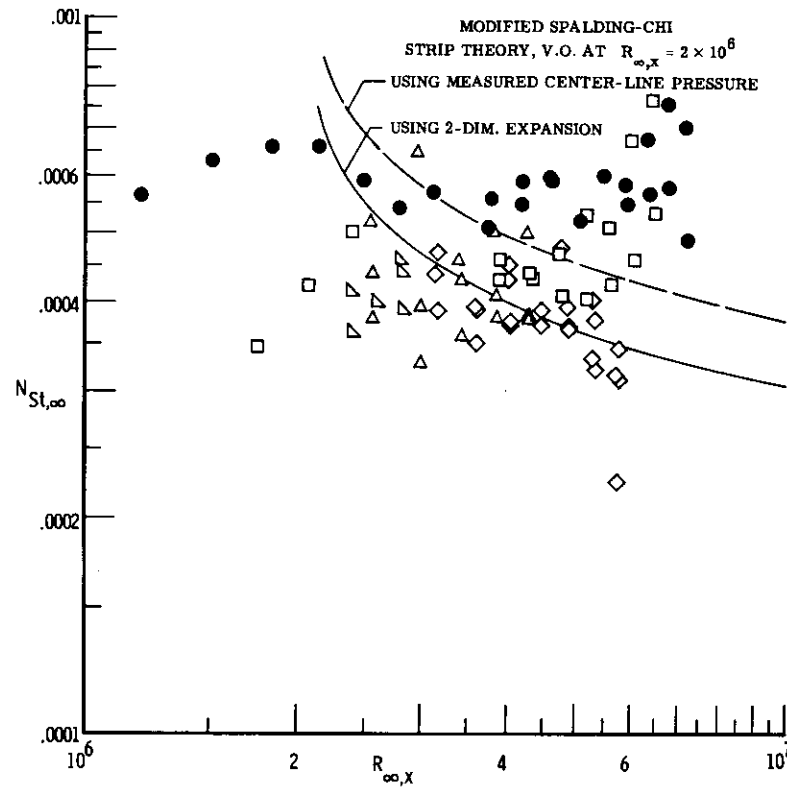


Figure 12.- Heat transfer and pressure distribution on leeward flat surface of sharp delta wing at $M_{\infty} = 6$. $\alpha = 5^{\circ}$; $\Lambda = 70^{\circ}$; $T_t = 960^{\circ} R$; $T_w/T_t = 0.6$; $R_{\infty,b} = 2.7 \times 10^6$; $b = 4.91$ in.; $R_{\infty,x_k} = 0.48 \times 10^6$.

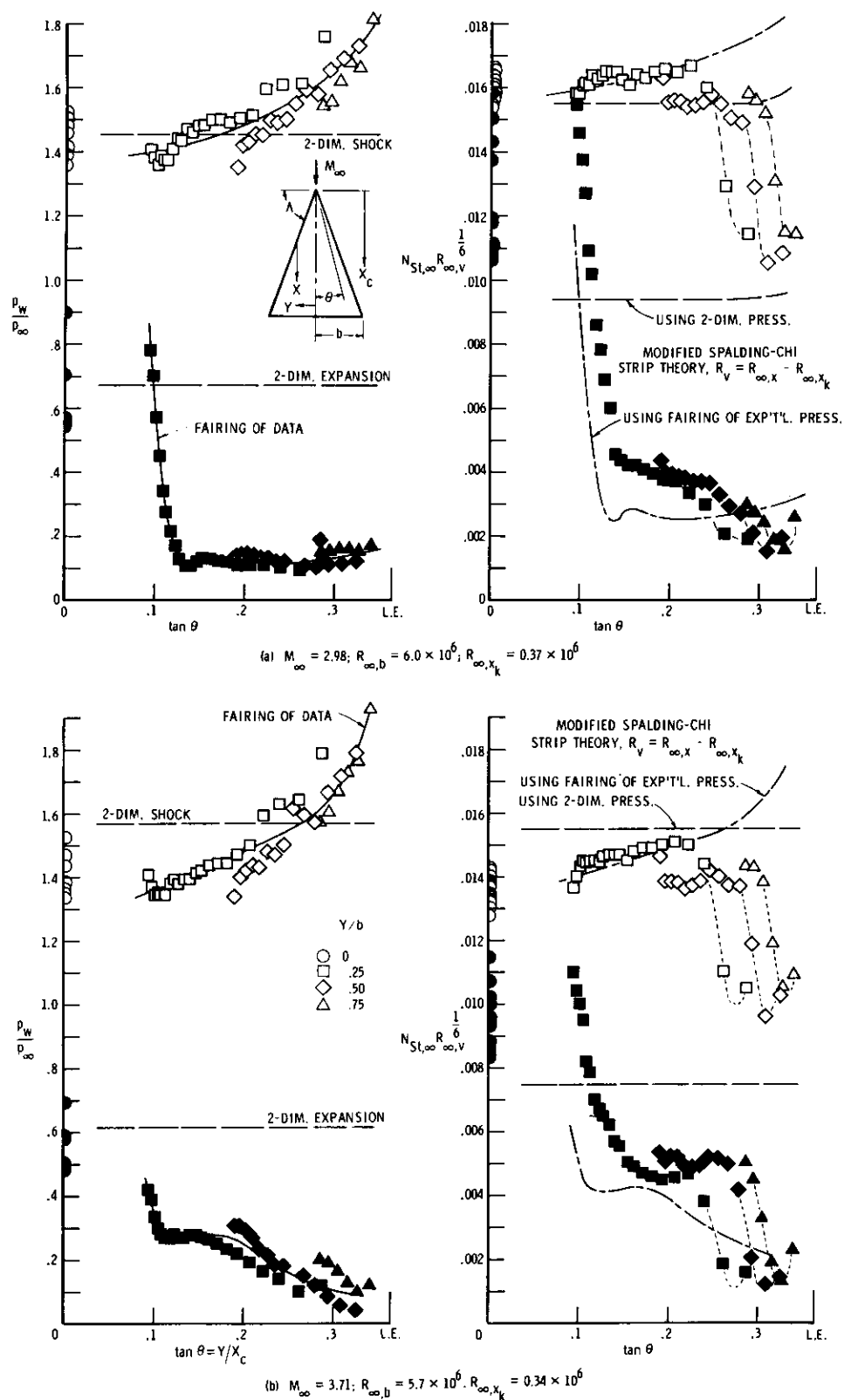
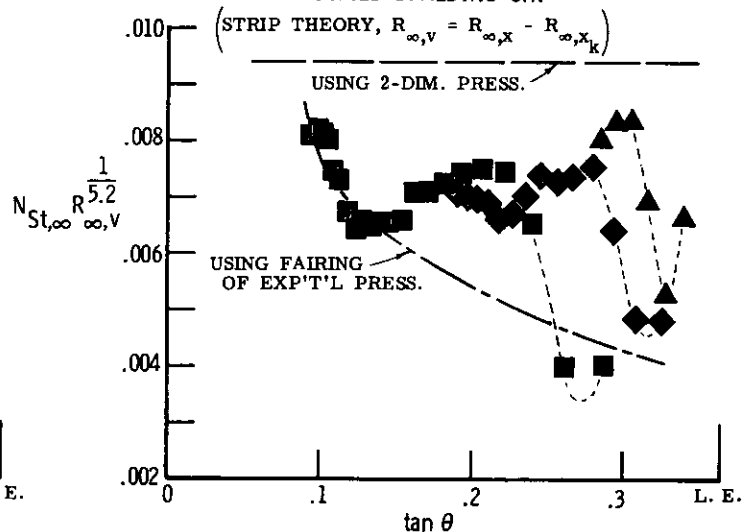
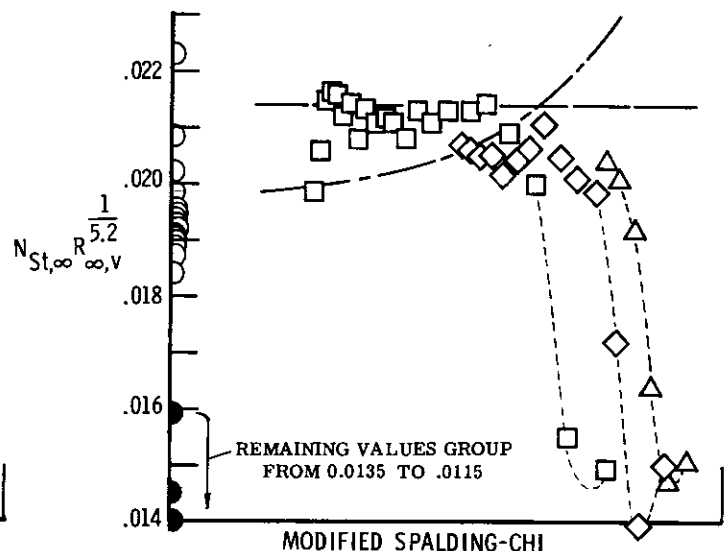
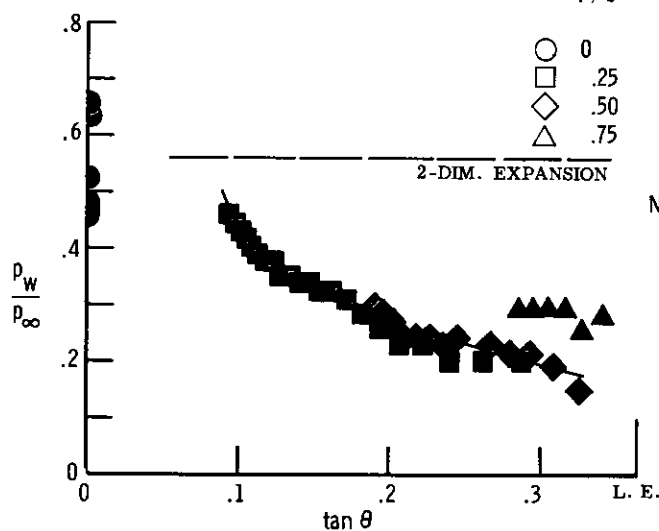
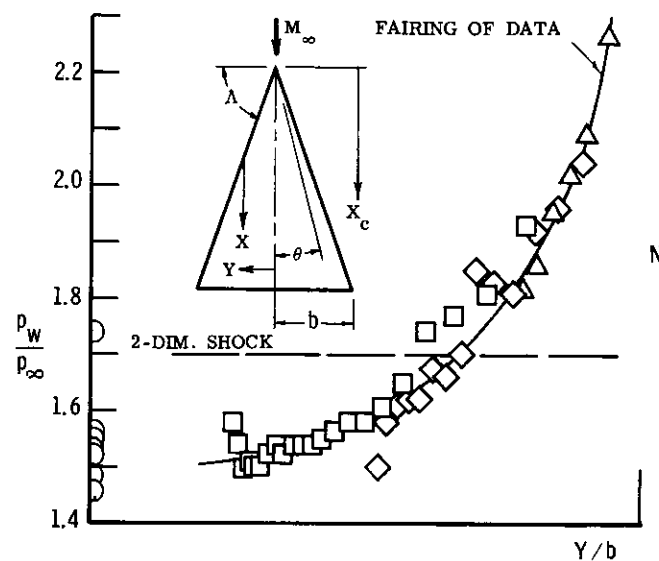


Figure 13.- Turbulent heat transfer on flat surface of sharp delta wing inclined windward and leeward. $\delta = 5^\circ$; leading-edge shock detached; $\Lambda = 70^\circ$; $T_w/T_t = 0.80 - .85$; $b = 12$ in.; $\lambda_n = 15^\circ$. Data from NASA TN D-3644.



(c) $M_\infty = 4.44$; $R_{\infty,b} = 5.8 \times 10^6$ $R_{\infty,x_k} = 0.35 \times 10^6$

Figure 13.- Concluded.